Origin of Unidentified Structures in Resonant Dissociative Photoionization of H_2

I. Sánchez and F. Martín

Departamento de Química, C-9, Universidad Autónoma de Madrid, 28049 Madrid, Spain
(Received 30 May 1997)

We present theoretical evidence that strong interference effects between resonant and nonresonant amplitudes are responsible for unidentified peaks observed in recent experiments on dissociative photoionization of H_2. We show that, at photon energies smaller than 27 eV, the various peaks can be explained in terms of a single $^1\Sigma_u^+$ doubly excited state. [S0031-9007(97)03889-1]

Dissociative photoionization of H_2 is the process in which a photon breaks the molecule into three fragments: $H + H^+ + e^-$. It plays a fundamental role in interstellar clouds, planetary atmospheres, and plasma physics. Historically, the first investigations of dissociative ionization were performed in the early 1970s (see Ref. [1] for references of this period). Experimental evidence of resonance effects was obtained by Strathdee and Browning [2] who observed a pronounced peak in the kinetic energy distribution (KED) spectra that they attributed to the lowest $^1\Sigma_u^+$ doubly excited state of H_2. This interpretation was later confirmed by theoretical calculations [3,4] that were able to reproduce both the position and the qualitative shape of the resonance peak.

Despite the apparent simplicity of H_2 and the number of experimental works devoted to it in the last 20 years, our knowledge of this fundamental process is far from being complete. For instance, very recently, Ito, Hall, and Ukai [1] have reported the existence of several peaks in the KED of protons that have been neither observed in previous works nor predicted theoretically. Surprisingly, the positions of these peaks do not seem to correspond to any known resonant state of H_2. In a different experimental approach, He *et al.* [5] have observed some structure in the zero ion kinetic energy spectrum of H_2 in the region of low photon energies. The use of simple energy conservation arguments leads to the conclusion that this low energy structure might correspond to a $^1\Sigma_g^+$ doubly excited state. However, this is very puzzling because the dipolar model, which should be valid for the radiation intensities reported in that work, does not allow excitation of a $^1\Sigma_g^+$ resonance. Finally, Latimer *et al.* [6] have determined, from their measured KED spectra, autoionization widths for the lowest $^1\Sigma_u^+$ and $^1\Pi_u$ doubly excited states of H_2 in clear disagreement with the most recent theoretical calculations [7,8].

In this Letter we show that all these experimental observations are the result of the strong interference between resonant and nonresonant dissociation processes. For this purpose, we closely follow the pioneering ideas of Bardsley [9] and Hazi, Rescigno, and Kurilla [10]. These authors have provided an appropriate theoretical framework to describe the electronic and nuclear motions, and the in-

terference between them. In the present paper we have generalized this theoretical approach to study dissociative photoionization of H_2. We make use of *B*-spline functions [11] to represent both the electronic and nuclear wave functions. The advantage of using B splines is that one can apply algebraic techniques to solve the complicated systems of integrodifferential equations that arise from the theory. This is essential to account for interference effects not included in previous theoretical works and to explain the experimental findings.

In the dipole approximation, the cross section for ionization from the initial state $\Psi_{g\nu}(\mathbf{r}, R)$ is given (in atomic units) by [12]

$$\sigma_{\alpha\nu}(E) = \frac{4\pi^2\omega}{3c} \sum_{plm} \left| \int dR \langle \Psi_{g\nu}|\mathbf{e}_p \cdot \mathbf{D}|\Psi^+_{\alpha\nu lmE}\rangle \right|^2,$$

$$(1)$$

where g and ν indicate the initial electronic and vibrational states, respectively, $\hbar\omega$ is the photon energy, $\mathbf{e}_p$ is the photon polarization vector, $\mathbf{D}$ is either $\mathbf{r}_1 + \mathbf{r}_2$ (length gauge) or $(\nabla_1 + \nabla_2)/\hbar\omega$ (velocity gauge), and $\Psi^+_{\alpha\nu lmE}(\mathbf{r}, R)$ is the final state. In the latter state, the superscript $+$ indicates the usual outgoing boundary conditions in electron-molecule scattering, l and m are the angular momentum quantum numbers of the ejected electron, $E = W_{g\nu} + \hbar\omega$ with $W_{g\nu}$ the total energy of the molecule in the initial state, and α and ν denote, respectively, the electronic and vibrational states of the residual molecular ion. The label $\mathbf{r}$ is used for electronic coordinates, and R is the internuclear distance. In Eq. (1) we have factored out the rotational wave functions and averaged upon all possible orientations. Next we assume that the initial state is well described in the framework of the Born-Oppenheimer (BO) approximation, i.e., $\Psi_{g\nu}(\mathbf{r}, R) = \psi_g(\mathbf{r}, R)\chi_\nu(R)$, where ψ_g is the initial electronic state and χ_ν is the nuclear wave function calculated in the potential energy curve $E_g(R)$ associated with ψ_g. In the present work, ψ_g is the $X^1\Sigma_g^+$ electronic state of H_2 and χ_ν the vibrational state with $\nu = 0$. Therefore, application of the dipole selection rules to Eq. (1) implies that only electronic states of $^1\Sigma_u^+$ and $^1\Pi_u$ symmetries will be populated.

In the resonance region, the final state $\Psi^+_{\alpha v l m E}$ has contributions from the nonresonant background as well as from the resonant doubly excited states. This implies that a realistic description of the nuclear wave function must take into account the interference effects between the direct ionization and autoionization processes. Here we assume that (i) ionization leaves the residual electron

in a $1s\sigma_g$ orbital of H_2^+, and (ii) the coupling between resonant and nonresonant states is due to electronic interaction only. We call ϵ the kinetic energy of the outgoing electron, $\phi_r(\mathbf{r}, R)$ the resonant states of energy $E_r(R)$, and $\psi^{0+}_{\alpha l m \epsilon}(\mathbf{r}, R)$ the nonresonant continuum states in which the former are embedded. Then the final state wave function can be written [13]

$$\Psi^+_{\alpha v l E}(\mathbf{r}, R) = \sum_{r'} \phi_{r'}(\mathbf{r}, R) \xi^{r'}_{\alpha v l E}(R) + \psi^{0+}_{\alpha l \epsilon}(\mathbf{r}, R) \chi_v(R) + \lim_{\eta \to 0} \sum_{r'} \sum_{\alpha' l'} \sumint_{v'} \sumint dE' \frac{1}{E - E' + i\eta}$$
$$\times \int dR' \, V^{r'*}_{\alpha' v' l' E'}(R') \xi^{r'}_{\alpha v l E}(R') \psi^{0+}_{\alpha' l' \epsilon'}(\mathbf{r}, R) \chi_{v'}(R), \tag{2}$$

where

$$V^r_{\alpha v l E}(R) = \langle \phi_r | \mathcal{H}_{el} | \psi^{0+}_{\alpha l \epsilon} \rangle \chi_v(R) \tag{3}$$

and $\mathcal{H}_{el}$ is the electronic Hamiltonian. Note that we have dropped the index m because $^1\Sigma_u^+$ and $^1\Pi_u$ continuum states, which have different m, are not coupled. In Eqs. (2) and (3), χ_v is the nuclear wave-function solution

of the equation

$$[T(R) + E_{H_2^+}(R) - W_v]\chi_v(R) = 0, \tag{4}$$

where T is the relative kinetic energy of the nuclei, $E_{H_2^+}(R)$ is the potential energy curve of the $X^2\Sigma_g^+$ state of H_2^+, W_v is the energy of the residual H_2^+ ion, $E = \epsilon + W_v$, and $\xi^r_{\alpha v l E}$ is the solution of [9,10,13]

$$[E - E_r(R) - T(R)]\xi^r_{\alpha v l E}(R) = V^r_{\alpha v l E}(R) + \lim_{\eta \to 0} \sum_{r'} \sum_{\alpha' l'} \sumint_{v'} \sumint dE' \frac{V^r_{\alpha' v' l' E'}(R)}{E - E' + i\eta}$$
$$\times \int dR' \, V^{r'*}_{\alpha' v' l' E'}(R') \xi^{r'}_{\alpha v l E}(R'). \tag{5}$$

The latter equation represents the nuclear motion when the electrons are in the quasistationary state ϕ_r. The matrix element in Eq. (3) represents the coupling between the resonance ϕ_r and the nonresonant wave function $\psi^{0+}_{\alpha l \epsilon}$ and vibrational state v. Hence, the two terms in the right-hand side of Eq. (5) are the result of the autoionizing character of the ϕ_r state. In particular, the last term represents the decay of the resonant state to the adjacent electronic continuum. This term, as well as the last one in Eq. (2), is nonlocal due to the presence of the $\xi^r_{\alpha v l E}$ functions, and it can be split into a delta function term and a principal value term. We emphasize that Eqs. (2) and (5) are exact within the BO approximation [10,13]. The main difference between Eq. (5) and those derived by Bardsley [9] and Hazi, Rescigno, and Kurilla [10] is that we have employed the usual partial wave expansion of electron-molecule scattering while these authors make use of a single molecular continuum. In previous works [3,10], Eq. (5) is further simplified by using a local approximation for the last term. Also, contributions arising from the last term in Eq. (2) are usually neglected (e.g., see [3]). In the present Letter, all the nonlocal terms have been evaluated. The resonant wave functions ϕ_r and the continuum wave functions $\psi^{0+}_{\alpha l \epsilon}$ have been taken from Refs. [8,14], where they were used to obtain resonance parameters and photoionization cross sections in the fixed nuclei approximation. Briefly, the resonant wave functions ϕ_r were

obtained by diagonalizing the H_2 Hamiltonian in a basis of $\simeq 200$ configurations built from B-spline functions of order eight defined in a box of 60 a.u. and with angular momenta up to $l_{max} = 8$. Here we only consider the lowest $^1\Sigma_u^+$ and $^1\Pi_u$ doubly excited states. The nonresonant wave functions $\psi^{0+}_{\alpha l \epsilon}$ describe a bound electron in the $1s\sigma_g$ orbital of H_2^+ and a continuum electron with angular momentum up to $l = 7$. They were evaluated using the L^2 close-coupling method [15], which allows for interchannel coupling between different partial waves and yields the correct outgoing asymptotic behavior (see Refs. [8,14] for details). In Ref. [8] we have shown that these wave functions lead to an accurate description of resonant electronic properties. The ground state of H_2 has been taken from Ref. [14]. The initial and final vibrational states have been obtained by diagonalizing the corresponding vibrational Schrödinger equations in a basis of B-spline functions of order eight defined in a box of 12 a.u. The most difficult part is the evaluation of the $\xi^r_{\alpha l v E}$ wave functions from Eq. (5). This equation is transformed into a system of linear equations by expanding $\xi^r_{\alpha l v E}$ in a basis built from the B-spline basis just mentioned (see Ref. [13] for details). All energy integrals in Eqs. (2) and (5) have been evaluated using quadrature procedures consistent with our B-spline basis [13].

The resonant states considered in this work lie above the ionization threshold at short and intermediate R (see

Fig. 1). At $R = R_c$, their energies cross the ionization threshold and the states lose their autoionizing character. For instance, the lowest $^1\Sigma_u^+$ resonance, which is mainly described by a $2p\sigma_u2s\sigma_g$ configuration, crosses the $1s\sigma_g$ ionization threshold at $R_c \simeq 4.1$ a.u. As R increases, the resonant states cross the $1s\sigma_g nl\lambda$ Rydberg series and dissociate into H($1s$) + H($n = 2$). For $R > 6$ a.u., we have used the diabatic potential energy curves calculated in Ref. [16]. These curves tend to the correct dissociation limit and have been smoothly connected to our results for $R \leq 5.0$ a.u. Since autoionization below the threshold is not allowed, all matrix elements involving the interaction between these diabatic states and the $\psi_{\alpha l\epsilon}^{0+}$ states have been made zero beyond R_c. Also, in Eqs. (2) and (5), we have excluded the bound electronic states because contributions from the latter to the ionization process is expected to be negligible.

We show in Fig. 2 the calculated kinetic energy distribution for the $^1\Sigma_u^+$ symmetry at a photon energy $\hbar\omega = 27$ eV. This is compared with the spectrum measured by Ito, Hall, and Ukai [1] for protons observed at 0° with respect to the polarization vector of the incident radiation (note that for this observation angle, only the $^1\Sigma_u^+$ continuum is populated). Since the measurements are not given in an absolute scale, we have normalized the spectrum to the calculated value at 3 eV. In the absence of resonant effects, the cross section should decrease almost exponentially as the proton energy increases [17]. Figure 2 shows the existence of two well defined peaks at $\simeq 1.5$ and 3 eV. The origin of the high energy peak has been explained by Kirby *et al.* [3] using a local approximation and a wave function that only included the first resonant term in Eq. (2). The resonant contribution resulting from our calculations (see Fig. 2) agrees qualitatively with their results. However, note that the present resonant contribution includes the first and third terms in Eq. (2), and that the importance of both terms is comparable [13]. The low energy peak in Fig. 2 has been first observed by Ito, Hall, and Ukai [1], and it is well reproduced in our calculations. This peak, which could not be assigned in Ref. [1], is also apparent at higher photon energies [13].
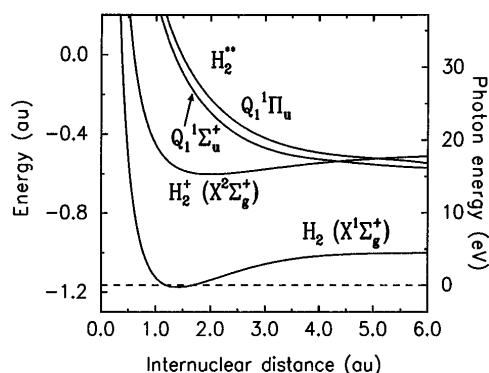
Figure 2 also shows the nonresonant contribution obtained by keeping only the second term in Eq. (2). The latter contribution exhibits the typical exponential decay of a KED spectra far from the resonance region. It can be observed that a simple incoherent addition of the resonant and nonresonant contributions does not lead to the peak at 1.5 eV. Therefore, it is clear that the origin of such a peak lies in the strong interference between the amplitudes associated with the resonant and nonresonant parts of the wave functions. Although the existence of interferences effects is not surprising (e.g., they are the basis of the Fano profiles observed in atomic photoelectron spectroscopy), the large magnitude of the additional peaks in the KED spectra is quite unexpected. Indeed, they can be even more pronounced than the resonance peak itself. The fact that these additional structures are not very far from the region where the cross section decreases very rapidly may explain why they have remained undetected for a long time. The presence of these peaks seems to be a general phenomena as illustrated by our results for H_2 and D_2 in a broad range of photon energies (see Ref. [13]). Hence, the usual semiclassical picture in which the resonance is populated more or less efficiently and then the nuclei separate as the superexcited molecule slides down the potential curve $E_r(R)$ towards larger internuclear separations is not substantiated. In particular, discrepancies between theoretical and experimental autoionization widths [6] might be due to the use of this semiclassical model to extract the widths from the measured spectra. In contrast with the $^1\Sigma_u^+$ symmetry and despite the fact that the lowest $^1\Pi_u$ doubly excited state is included explicitly in the present calculations, no structure is observed for the $^1\Pi_u$ channel at photon energies $\hbar\omega \leq 27$ eV. This is consistent with the experimental results obtained for protons ejected at 90° [1].

We have integrated from 0 to $\mathcal{E}_{max}$ the KED spectra (as the one shown in Fig. 2) for the $^1\Sigma_u^+$ and $^1\Pi_u$ symmetries and for various photon energies. $\mathcal{E}_{max}$ is the maximum energy available for partitioning between nuclear motion

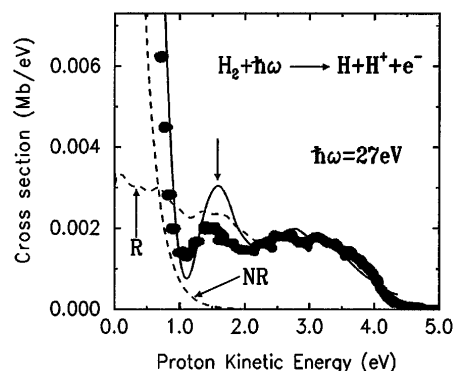FIG. 1. Potential energy curves for H_2 and H_2^+.

FIG. 2. KED spectrum of H_2 for a photon energy of 27 eV. Full line: present results; circles: experimental results from Ref. [1]; dashed lines: (R) resonant and (NR) nonresonant contributions. The arrow indicates the peak unidentified in previous works.
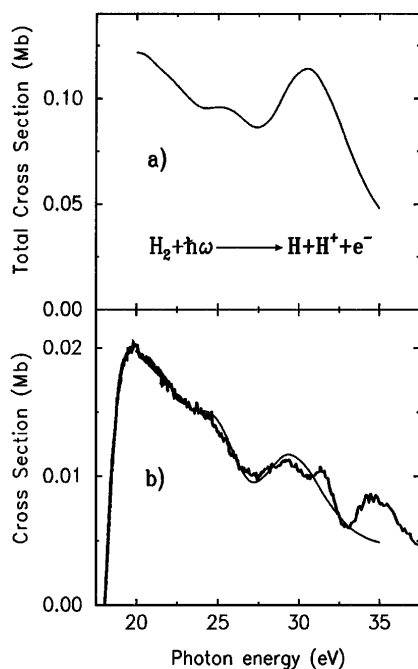
FIG. 3. Dissociative photoionization cross section of H_2 as a function of photon energy. (a) Present total cross section. (b) Results for protons with energy smaller than 0.04 eV; thick line: experiment of Ref. [5] for protons with energy smaller than 0.01 eV (normalized to the theory at $\hbar\omega = 20$ eV).

and photoelectron, $\mathcal{E}_{\max} = W_{g\nu} + \hbar\omega - E_{H_2^+}(\infty)$. The resulting total dissociative photoionization cross sections are shown in Fig. 3(a). Figure 3(b) includes results obtained by stopping the integration in $\mathcal{E}_f = 0.08$ eV ($\mathcal{E}_f \ll \mathcal{E}_{\max}$). As for the KED spectra, the peaks observed here come from the $^1\Sigma_u^+$ channel and practically no structure is obtained in the $^1\Pi_u$ channel. For the purpose of discussion, we have also included in Fig. 3 the zero kinetic energy spectrum measured by He *et al.* [5] normalized to our results at $\hbar\omega = 20$ eV. The latter has been obtained in arbitrary units by collecting protons with energy smaller than 0.01 eV. We have not attempted to obtain a "zero energy" spectrum due to the large number of points required near the dissociation threshold. However, one can see that in both cases we obtain two peaks almost in the same positions as in the experiment. Furthermore, for $\mathcal{E}_f = 0.08$, the shapes of both structures tend to the experimental ones. The peak at higher energies appear at $\hbar\omega \simeq 30$ eV, which is the energy required to populate the lowest $^1\Sigma_u^+$ resonance state assuming that this state is formed in a Franck-Condon transition from the ground state [5]. The peak at lower energies is the result of the interference with the nonresonant background. We do not need to include any additional $^1\Sigma_g^+$ resonance state to account for the low energy peak. As in the case of the KED spectra, the existence of several structures in the spectrum at low photon energies can be explained in terms of the interference between the lowest $^1\Sigma_u^+$ doubly excited state and the nonresonant background. The peaks observed at $\hbar\omega \geq 30$ eV correspond to resonant states not included in the present calculations.

In conclusion, we have shown the existence of strong interference effects between resonant and nonresonant amplitudes that are responsible for the appearance of unexpected structures in dissociative ionization spectra of H_2. Since the interferences are the result of the quantal behavior of both electrons and nuclei, no semiclassical model can account for the experimental findings. Our analysis shows that the usual one-to-one correspondence between observed peaks and resonances is no longer valid to interpret dissociative photoionization spectra. At the photon energies investigated here, the various peaks observed experimentally can be explained in terms of a single $^1\Sigma_u^+$ doubly excited state.

[1] K. Ito, R. I. Hall, and M. Ukai, J. Chem. Phys. **104**, 8449 (1996).

[2] S. Strathdee and R. Browning, J. Phys. B **12**, 1789 (1979).

[3] K. Kirby, T. Uzer, A. C. Allison, and A. Dalgarno, J. Chem. Phys. **75**, 2820 (1981).

[4] S. Kanfer and M. Shapiro, J. Phys. B **16**, L655 (1983).

[5] Z. X. He, J. N. Cutler, S. H. Southworth, L. R. Hughey, and J. A. R. Samson, J. Chem. Phys. **103**, 3912 (1995).

[6] C. J. Latimer *et al.,* J. Phys. B **26**, L595 (1993); J. Geddes *et al., ibid.* **27**, 2961 (1994); C. J. Latimer *et al., ibid.* **29**, 6113 (1996).

[7] I. Shimamura, C. J. Noble, and P. G. Burke, Phys. Rev. A **41**, 3545 (1990); J. Tennyson, At. Data Nucl. Data Tables **64**, 253 (1996).

[8] I. Sánchez and F. Martín, J. Chem. Phys. **106**, 7720 (1997).

[9] J. N. Bardsley, J. Phys. B **1**, 349 (1968).

[10] A. U. Hazi, T. N. Rescigno, and M. Kurilla, Phys. Rev. A **23**, 1089 (1981).

[11] C. de Boor, *A Practical Guide to Splines* (Springer, New York, 1978).

[12] I. Cacelli, V. Carravetta, A. Rizzo, and R. Moccia, Phys. Rep. **205**, 283 (1991).

[13] I. Sánchez and F. Martín (to be published).

[14] I. Sánchez and F. Martín, J. Phys. B **30**, 679 (1997).

[15] F. Martín, Phys. Rev. A **48**, 331 (1993); M. Cortés and F. Martín, J. Phys. B **27**, 5741 (1994).

[16] F. Borondo, A. Macías, and A. Riera, J. Chem. Phys. **74**, 6126 (1981).

[17] S. V. ONeil and W. P. Reinhardt, J. Chem. Phys. **69**, 2126 (1978).